Polymer Chemistry

PAPER

View Article Online
View Journal | View Issue

Cite this: *Polym. Chem.*, 2016, **7**, 6805

Facile fabrication of a 3D electrospun fibrous mat by ice-templating for a tumor spheroid culture†

Yanru Li, Lingbo Sun, Hongxia Fu and Xinrui Duan*

Received 2nd October 2016,
Accepted 13th October 2016

DOI: 10.1039/c6py01718e

www.rsc.org/polymers

Electrospinning technology is a simple, convenient, and cost-effective method to fabricate nano/micro fibrous materials. Electrospun fibers are generally collected as a two-dimensional (2D) mat, which lacks a complex and macroscopic three-dimensional (3D) structure. In this work, we fabricated polycaprolactone (PCL) electrospun fibrous materials with small wells (wPCL) by using icy balls as templates. A cooling system was designed and incorporated into the electrospinning setup to achieve our goal. The size and distances between the wells can be easily controlled by a simple water spotting process. When we added cell culture medium droplets into the fabricated wells and placed them upside down, we found that the structure could stabilize the droplets against small mechanical shocks and perturbations, which makes it a good platform for a 3D spheroid culture by the hanging droplet method. Furthermore, the fibrous nature of the electrospun mat ensured the better exchange of O_2 and CO_2 between the droplet and surrounding environment. We also demonstrated that the cubic and triangle shaped 3D electrospun fibrous mat can be fabricated using a similar methodology. Our results indicate that electrospinning technology involving ice-templated collection is a mild and straightforward way to fabricate 3D electrospun materials and can be readily used for a 3D cell culture.

Introduction

Electrospinning technology is a simple, convenient, and cost-effective method to fabricate nano/micro fibrous materials with a large surface area, wide selection of materials, suitable surface chemistries, and controllable mechanical properties.[1,2] Since Formhals first reported electrospinning in 1934,[3] it has been revived because of its potential to produce ultrafine nanofibers from a wealth of organic polymers.[4,5] It has broad applications in superhydrophobic surface preparation,[6] biosensing,[7] drug delivery,[8] and tissue engineering.[9] Electrospun fibers are generally collected as a two-dimensional (2D) mat, which has randomly arranged structures. The 2D fibrous mat lacks a complex and macroscopic three-dimensional (3D) structure, which has greatly limited its application. It is important to fabricate electrospun fibrous assemblies with controllable three-dimensional (3D) structures in order to realize the potential of such materials.[10] Several approaches have been developed for fabricating 3D fibrous materials such as charge repulsion,[11,12] wet collector,[13] assistance of an inert gas,[14] and template-assisted collection.[15–18] Only template-assisted collection could produce controllable 3D electrospun structures. Different shapes of the metallic collectors or patterned silicic templates were fabricated first, and electrospun fibers were collected on the surface of the templates to generate 3D fibrous materials with various different structures. Instead of the metallic or silicic template, we presume that using ice with a definite shape as a 3D template would make the fabrication process much easier, since ice of various shapes can be easily obtained by freezing water and removing it from the electrospun fibrous mat by vacuum drying after electrospinning, which should avoid the complicated fabrication process of a template and existence of trace residues of metals. Indeed, it has been reported that randomly formed ice crystals with diameters in microns can be used to fabricate electrospun fibers with a large pore size to promote cell infiltration.[19,20]

In this work, we propose to fabricate polycaprolactone (PCL) electrospun fibrous materials with small wells with a defined shape and size (wPCL) by using icy balls as templates. A water droplet would perfectly fit in such wells. Comparing with the 2D surface, when the water droplet inflicts a mechanical shock or perturbation, this semi-spherical structure can greatly prevent the sliding of the droplet and the frictional force and capillary effect in the interface between the droplet and electrospun fibers could prevent the droplet to fall out of the fibrous mat. This could make our material perfectly fit in the application of hanging droplets for a 3D tumor spheroid

Key laboratory of analytical chemistry for life science of Shaanxi Province, School of Chemistry and Chemical Engineering, Shaanxi Normal University, Xi'an, Shaanxi, 710119, P. R. China. E-mail: duanxr@snnu.edu.cn

† Electronic supplementary information (ESI) available: Experimental details of a cubic and triangle PCL electrospun mat, polystyrene electrospun mat, general cell culture and MTT assay; Fig. S1–S5. See DOI: 10.1039/c6py01718e

culture, since the hanging droplets are susceptible to small mechanical shocks and perturbations. Furthermore, the fibrous nature of the electrospun mat ensured a better exchange of O_2 and CO_2 between the droplet and surrounding environment.[1]

Since the 3D cell culture was considered as a potential link to bridge the gap between 2D monolayer cultures and animal model studies, it has attracted a lot of attention.[21–25] Multicellular tumor spheroids are the most popular 3D cancer cell culture system and have been a useful tool for investigating specific microenvironment factors associated with tumor therapy, such as the mechanism of the action of chemotherapy and radiotherapy as well as drug screening.[26] Multicellular tumor spheroids are aggregates of cells, which are similar to the native tumors.[27] Several types of cell spheroid culture methods have been reported such as agitation-based approaches,[28] 3D scaffold and matrix based approaches,[29] microfluidic systems,[30,31] forced-floating,[32] and hanging drops.[33–35]

Among these methods, the hanging drop culture is the most popular method. It is cost-efficient and easy to operate, and has almost 100% reproducibility of producing one 3D spheroid per drop for numerous cell lines.[36] In this method, gravity pulled the cells to the bottom of a hanging droplet, which would start the natural organization of cell–cell attachment and the production of ECM.[33] Since hanging droplets on the 2D surface are susceptible to small mechanical shocks and lack stability against droplet spreading triggered by mechanical perturbations, a micro-ring structure was designed to improve stability by preventing droplet spreading on polystyrene hanging drop array plates.[35] In this method, a procedure for processing machinery is required and it is not a common technique in biology laboratories. By contrast, biologists are familiar with the electrospinning technique because of its wide application in tissue engineering.[1,9]

Our work showed that with a small modification in the electrospinning device and with the help of icy balls, 3D fibrous materials could be easily generated to serve as nice platforms for a tumor spheroid culture by the hanging drop method. In our study, we designed and prepared 3D electrospun PCL fibrous materials that had many wells with a controllable size, distance and pattern (namely PCL with wells, wPCL). As shown in Scheme 1, the whole preparation process was simple, cheap, and effective by using spherical ice on superhydrophobic aluminum foil as a fiber collector. At first, we prepared a superhydrophobic aluminum foil surface (Fig. S1†). Deionized (DI) water droplets were patterned on the superhydrophobic aluminum foil surface by directly pipetting DI water at specific spots (Scheme 1 inset image a). Secondly, we froze all water droplets to make spherical ice. Thus the size and distance of the wells easily varies according to need. Finally, we fabricated the PCL fibrous mat on top of the icy balls. These icy balls served as a mold to create wells on PCL fibrous materials. Later we used wPCL for a tumor spheroid culture. Droplets of the cell suspension solution were transferred into each well. The shape of the wells on our material could ensure the stability of the liquid drop and minimize the adverse influence on tumor spheroids (Scheme 1, inset image b). By using the hanging droplet method, MCF-7 cells were seeded in wells and the spheroids were formed after 24 h of incubation (Scheme 1, inset image c). Our study presents a mild and straightforward method to produce spheroids.

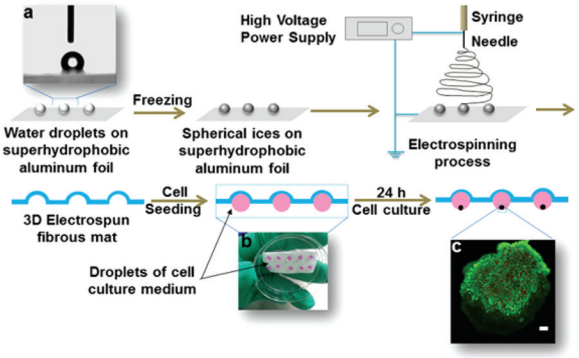

Scheme 1 Schematic representation of the procedure for the production of the wPCL fibrous mat and multicellular tumor spheroids. Inset images: (a) water droplet on superhydrophobic aluminum foil; (b) droplets of cell culture medium with cells at the bottom of the wPCL fibrous mat. (c) Fluorescence image of the formed spheroid with live (green)/dead (red) staining by calcein-AM and PI respectively. Scale bar is 100 microns.

Experimental section

Materials and methods

Polycaprolactone (PCL), poly(diallyldimethylammonium chloride) (PDDA), and sodium 4-styrenesulfonate (PSS) were purchased from Sigma-Aldrich. Dulbecco's modified Eagle's medium (DMEM) and other medium components were purchased from Sigma-Aldrich. Fetal bovine serum (FBS) was obtained from Hyclone laboratories Inc. 1,1,1,3,3,3-Hexafluoro-2-propanol (HFIP) and perfluorooctanoate (PFO) were obtained from J&K Scientific Ltd. Propidium Iodide (PI, Cell Apoptosis PI Detection Kit), doxorubicin (Dox), paraformaldehyde, ActinGreen (phalloidin-FITC solution, 200 U mL^{-1}), and DAPI (4,6-diamidino-2-phenylindole, ready-to-use solution) were purchased from Nanjing Key GEN Biotech. Co. Ltd. Calcein-AM was obtained from Fan bo Biochemicals Co. Ltd. Methyl alcohol and chloroform were obtained from Sinopharm chemical Reagent Co. Ltd. Millipore Simplicity 185 purification unit purified water (18.2 MΩ cm) was used for rinsing and preparing all aqueous solutions. All other reagents were obtained commercially and used without further purification. Scanning electron microscopy (SEM, FEI Quanta 200 or Hitachi TM3030) was used to observe the morphology of electrospun fibers. All samples were dried under vacuum overnight and sputter coated with gold for 80 s before imaging.

Preparation of superhydrophobic aluminum surface

The superhydrophobic aluminum foil was prepared by following a reported process.[37] The square 4 × 4 cm^2 aluminum foil was ultrasonically cleaned for 2 min each in deionized water, ethanol, chloroform, and acetone to remove impurities. Afterward, the cleaned aluminum foil was etched at room temperature in 2.5 M hydrochloric acid for 4 min and then was immersed for 20 min in boiling deionized water and finally dried with nitrogen gas flow. Subsequently, a $(PDDA/PSS)_{1.5}$ polyelectrolyte multilayer film was applied to the rough aluminum foil by following a literature procedure[38] that alternately dipped the aluminum foil for 20 min into PDDA (1.0 mg mL^{-1}, with 1.0 M NaCl present) and PSS (1.0 mg mL^{-1}, with 1.0 M NaCl present) aqueous solutions, and then into PDDA again, with a water rinse and nitrogen dry included after each dipping. Finally, this substrate was dipped into PFO (0.1 M) aqueous solutions for 3 min before rinsing with water and drying under nitrogen gas flow.

Typical electrospinning process

PCL was dissolved in HFIP and a mixed solvent of chloroform and methanol with a 7 to 1 volume ratio. After 12 hours of stirring at room temperature, 0.08, 0.1, and 0.12 g mL^{-1} PCL solutions in HFIP were formed, and 0.12, 0.15 and 0.18 g mL^{-1} PCL solutions in a mixed solvent of chloroform and methanol with a 7 to 1 volume ratio were made respectively. The electrospinning was performed by a home-made electrospinning setup. The polymer solution was transferred to a 2 mL glass syringe connected to a 21G blunt stainless steel needle, which was connected to a high-voltage supply. The polymer solution was dispensed utilizing a syringe pump (LSP01-1A, Longer pump, Baoding, Hebei, China) at a constant flow rate of 1 mL h^{-1} in a cubic chamber. The humidity of the chamber was monitored by a digital humidity and temperature thermometer (GM1361) controlled under 15% relative humidity by dry air flow from an air compressor (OTS-800, Taizhou, China). The temperature of the collector was controlled under −3 °C by the cooling system including an aluminum cool water block, water circulating pump, and ice-salt bath. 5 μL of deionized (DI) water was patterned on the aluminum foil surface by directly pipetting at a specific spot. Then the aluminum foil was kept in the freezer for 3–5 min to form spherical ice. Finally, the aluminum foil was transferred on the cool water block as used as a ground collector. The ground aluminum foil collector was placed under the tip of the needle with a distance of 10.5 cm. Electrospinning of the PCL solution was carried out by applying a positive voltage of 5–8 kV between the needle tip and the collector *via* high voltage power supply (DW-P303, Tianjin Dong Wen High Voltage Power Supply Co., Ltd, Tianjin, China) for around 1 hour. The resulting PCL fibrous mat with wells (wPCL) was kept overnight in a vacuum-dry oven in order to remove residual solvents. The wPCL fibrous mat was sterilized by immersing it in 75% ethanol for 30 min followed by UV irradiation for 30 min in a laminar flow hood before cell seeding.

Aqueous droplet stability test

Three cell culture medium (DMEM + 10% FBS) droplets (5 μL for each droplet) were carefully added on top of each material. The material with the cell culture medium droplets was extremely carefully placed and slightly glued upside down onto a 1.5 mL cap-free Eppendorf tube. Later the whole setup was transferred into a centrifuge (Fei Ge GL-16G-II, ShangHai Anting Scientific Instrument Factory, Shanghai, China) for a stability test under different centrifugal forces up to 0–40*g* for 1 min. After centrifugation, the fallen cell culture medium droplets at the bottom of the Eppendorf tube were taken out by carefully pipetting them without touching the materials on the top. Cell culture medium droplets were weighed by using an Analytical Balance (Sartorius, BSA124S-CW) to evaluate the stability under different centrifugal forces.

Spheroid formation and drug screening

The wPCL fibrous mats were glued to the lid of the culture dish. The lower part of the culture dish was covered with 1% agarose to maintain the high humidity and minimize the evaporation of hanging cell medium droplets. 5 μL of MCF-7 cell suspensions of 8×10^6 cells per mL was dispensed in each well of the wPCL fibrous mats. Each experiment was performed in triplicate. Turning the fibrous mats upside down by covering the cell culture dish with the lid where the mat was fixed, the spheroids were allowed to form by gravitational force during 24 hours. Doxorubicin in the cell culture medium without phenol red was added to the droplets to give various final concentrations of 0, 0.1, 1, and 10 μg mL^{-1}, which were incubated for 24 h.

Laser confocal fluorescence microscope

For live/dead staining, spheroids were stained by using calcein-AM and PI. A volume of 2 μL of the staining solution containing 50 μM calcein-AM and 20 times diluted PI was added to the spheroids for 20 min at 37 °C. Dyes were excited at the 488 nm and 559 nm laser line respectively. Analyses of images were carried out by using ImageJ (1.48). For F-actin staining, MCF-7 cells and spheroids were fixed in 4% paraformaldehyde for 30 min and permeabilized with 0.1% Triton X-100 in PBS for 5 min. Afterwards, MCF-7 cells and spheroids were blocked by 100 mM glycine in PBS for 30 min. ActinGreen (5 μL of ActinGreen solution diluted in 200 μL of PBS) was added and incubated for 30 min. Cell nuclei were counterstained with DAPI for 10 min. All F-actin staining procedures were carried out at room temperature with PBS rinsing after each step. All samples were imaged by using an Olympus FV-1200 laser scanning confocal microscope.

Results and discussion

Scheme 2 shows a schematic representation of the electrospinning setup which consists of a high-voltage generator, a syringe pump, a collector, a cooling system, and an air compressor. The needle is connected to a high-voltage supply that

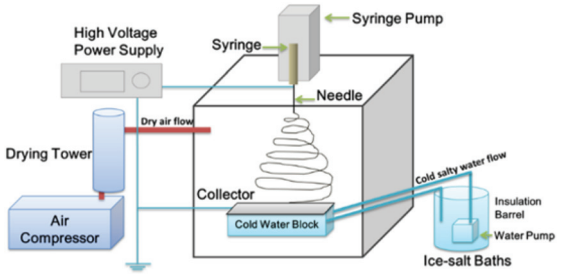

Scheme 2 Electrospinning setup for ice-templated 3D electrospinning.

is able to generate DC voltages up to 30 kV. Simultaneously, the spinneret is connected to a syringe in which the polymer solution is loaded. By using a syringe pump, the solution can be supplied at a constant and controllable rate. When a high voltage is applied, the small droplet of the polymer solution will experience electrostatic charges. Under the action of electrostatic charges, the liquid drop will be distorted into a conical object, which generally is known as the Taylor cone.[39,40] Once the strength of the electric field is sufficiently strong, with a voltage of 5–8 kV in our setup, charges built up on the surface of the droplet will overcome the surface tension of the polymer solution and thus induce the formation of a liquid jet. As the solvent is evaporating, the liquid jet is continuously extended to produce continuous ultrathin fibers, which are attracted by the low temperature ground collector placed at 10.5 cm underneath the needle. During electrospinning, a circulating water cooling system was added to the electrospinning setup that we previously reported[41,42] to control the temperature of the collector to prevent the melting of the icy balls. Meanwhile an air compressor coupled with a drying tower provided dry air flow to control the humidity of the surrounding environment.

To test our setup and also to gain electrospun fibers with homogeneous diameters, we studied the effects of the concentration of the polymer solution and solvents, which are the major parameters that affect the diameter of electrospun fibers.[39] We observed no significant difference between the effect of the concentration of PCL and the solvent on our modified electrospinning apparatus and a previously reported electrospinning setup.[39] Results are showed in Fig. S2.† We chose 0.15 g mL^{-1} PCL in a mixed solvent (chloroform : methanol = 7 : 1) and 0.10 g mL^{-1} PCL in HFIP to fabricate a wPCL fibrous mat by using spherical ice crystals on the superhydrophobic aluminum foil as fiber collectors. By controlling the humidity of the chamber under 15% relative humidity and the temperature of the collector under −3 °C, wPCL fibrous mats were fabricated. Fig. 1 shows the morphologies of the resulting electrospun materials. By contrast, 0.10 g mL^{-1} PCL solution in HFIP could fabricate uniform fibers on spherical ice at a low temperature with a smaller diameter which indicated a more compact fibrous mat. So we selected 0.10 g mL^{-1} PCL solution in HFIP for later experiments. Unlike the previously reported metallic or silicon template based 3D electrospun fabrication methods,[14–18] ice can be removed completely by vacuum drying, which will eliminate the possibility of contamination of metals or silicon in the resulting material.

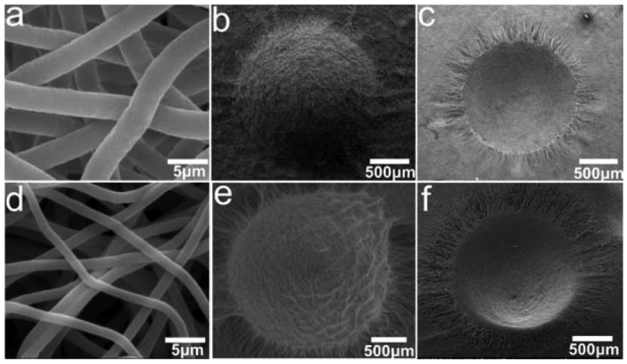

Fig. 1 (a–c) SEM images of electrospun fibers from 0.15 g mL^{-1} PCL in a mixed solvent (chloroform : methanol = 7 : 1) by using spherical ice on superhydrophobic aluminum foil as the fiber collector. (d–f) Morphology of electrospun fibers from 0.10 g mL^{-1} PCL in HFIP by using spherical ice on superhydrophobic aluminum foil as the fiber collector. SEM images (a) and (d) have the same magnification (10 000×). Rest of the images have the same magnification (100×).

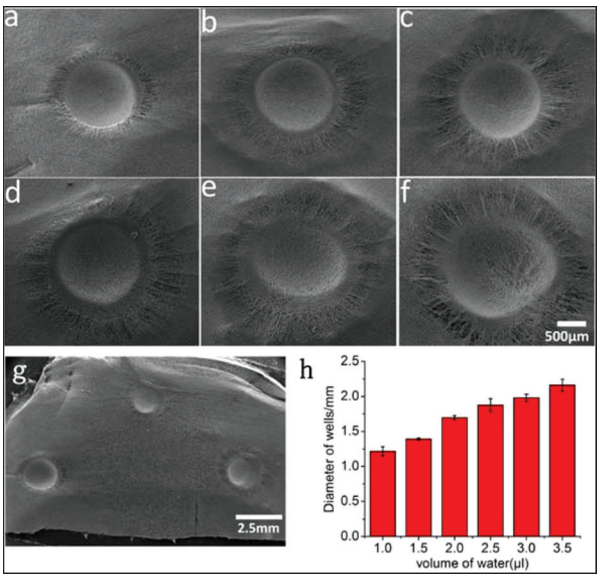

Fig. 2 SEM images of the electrospun fibrous mats, containing wells with different sizes (a–f) and distance (g) by using different volumes of spherical ice on superhydrophobic aluminum foil as the fiber collector. SEM images (a–f) have the same magnification (80×). The magnification of the SEM image (g) is 25×; (h) the plot of the diameter of the wells *versus* the volume of water. The error bars represent standard deviation (n = 3).

We froze drops of water to make spherical ice, so we were able to control the size and distance of the wells easily according to need. By using this technique, the wells could have the same or different sizes, distances and patterns synchronously. Fig. 2 shows that the wPCL fibrous mats produced are flexible and controllable. Fig. 2a–f show that the SEM images of the wPCL fibrous mats contain a series of various size controllable

wells by using different volumes of spherical ice on the superhydrophobic aluminum foil as fiber collectors. The spherical ice formed was from various volumes of water droplets, a, 1; b, 1.5; c, 2; d, 2.5; e, 3 and f, 3.5 μL. As is shown in Fig. 2h, the diameters of the wells depend on the volume of water droplets and have a variation that is directly proportional to the volume of water droplets. Fig. 2g shows that the SEM images of the wPCL fibrous mats can form specific patterns according to need, and that the distance between the well arrays is controllable.

In the hanging drop method, the stability of the aqueous droplet has an important effect on the tumor spheroid culture. To measure the difference in the stability of aqueous droplets on flat polystyrene (fPS), a plain PCL (pPCL) fibrous mat and wPCL materials, we added the same amount of cell culture medium (5 μL for each droplet) on the top of small pieces of each material. Each material was extremely carefully placed and slightly glued upside down onto a 1.5 mL cap-free Eppendorf tube. Later the whole setup was transferred into a centrifuge; we evaluated the stability by weighing the mass of falling liquid droplets at the bottom of the Eppendorf tube under different centrifugal forces. Under the same centrifugal force, the lighter the mass of falling droplets was, the better was the stability of the droplets. Each condition was processed in triplicate. It would also be ideal to test the performance of the electrospun polystyrene mat with wells and the electrospun PCL mat with wells for stabilizing droplets, unfortunately we did not get such materials from polystyrene. We found that the electrospun polystyrene mat was too soft and fluffy to keep the well structure. The images of such a polystyrene electrospun mat are showed in Fig. S3.† We suspected that the polystyrene electrospun mat was fluffy due to the repulsion between the electrospun nanofibers by the accumulation of negative charges under the influence of a strong electric field.[11,12] As shown in Fig. 3, cell culture medium droplets on the wPCL fibrous mat can endure a centrifugal force up to 16*g*. Meanwhile cell culture medium droplets that were hanging on the fPS or pPCL fibrous mat cannot endure such a high centrifugal force. These results indicated that aqueous droplets' stability on the wPCL fibrous mat was much better than fPS as well as the pPCL fibrous mat, which made it convenient to change the nutrient solution or add a drug to minimize the adverse influence on tumor spheroids. Compared with the 2D surface, when an aqueous droplet inflicts a mechanical shock or perturbation, our semi-sphere well structure can greatly prevent the sliding of the droplet and the frictional force and capillary effect in the interface between the aqueous droplet and electrospun fibers can prevent the droplet from falling out of the fibrous mat.

By using the hanging droplet technique, we seeded the same number of cells in each well of the wPCL fibrous mats to form spheroids. A volume of 5 μL of MCF-7 cell suspensions was dispensed in each well of the wPCL fibrous mats. Cell viability in the spheroids was visualized by using live/dead staining under laser confocal microscopy. Viable cells were stained green due to the conversion of calcein-AM to calcein by intercellular esterases, while nonviable cells that lost membrane integrity were stained red by PI. As shown in Fig. 4a, the spheroids were formed with diameters about 500 μm after 24 h. To further study the structural characteristics of multicellular spheroids, we compared the F-actin cytoskeletal organization in 2D monolayer MCF-7 cells and MCF-7 spheroids by ActinGreen staining. In Fig. 4b, 2D monolayer cultured MCF-7 cells have a flattened shape with the filopodia structure at the edges of the cells. However, as shown in Fig. 4c, the cells in the spheroid showed an F-action organization network of a typical 3D cell morphology. Cells have close contact with each other at the cellular junctions. This phenomenon indicates the formation of a 3D spheroid.[43]

We also explored the possibility of fabricating wells with other shapes in the electrospun mat. Electrospun mats with cubic and triangular shaped wells were fabricated based on a similar methodology and tested on the cell culture as well. The results are showed in Fig. S4.† Since the spheroids are formed at the bottom of the droplets, we did not observe any significant difference with the spherical shaped 3D electrospun mat.

As an *in vitro* model, multicellular spheroids provided an important link between monolayer cell cultures and animal experiments for effective drug screening. The use of multicellular spheroids is increasingly regarded as an essential step in drug development.[23] Dox was a conventional anticancer drug[44] which was used as a typical drug for therapeutic studies. For the drug screening assays, Dox was added in increasing doses in tumor spheroids. The influence of drug concentration on the cell viability was visualized using live/dead staining under laser confocal microscopy. The percentage of live cells in the

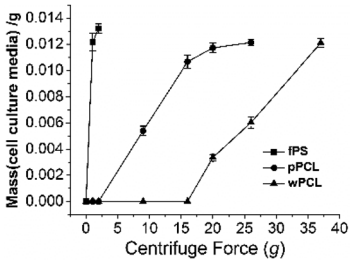

Fig. 3 Cell culture medium droplets' stability on the wPCL fibrous mat compared with flat polystyrene (fPS) and plain PCL (pPCL) fibrous mats under increasing centrifugal force. The error bars represent the standard deviation (n = 3).

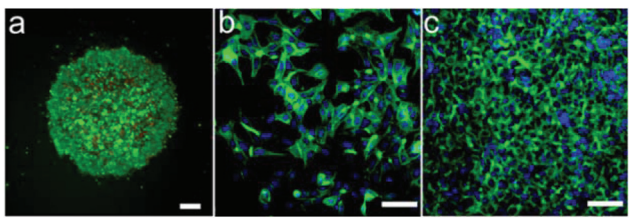

Fig. 4 Structure and morphology of 3D spheroids. (a) MCF-7 spheroid with live (green)/dead (red) staining (calcein-AM/PI); F-actin (green) was stained by ActinGreen and nuclei (blue) were stained by DAPI in (b) 2D monolayer MCF-7 cells and (c) MCF-7 spheroids. Scale bar is 100 microns.

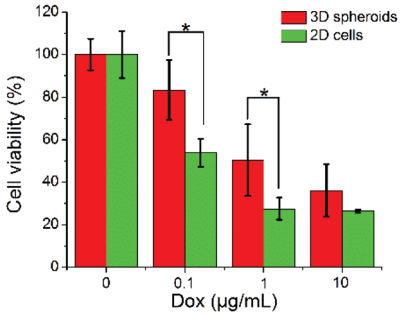

Fig. 5 Dose response of 3D MCF-7 spheroids and 2D monolayer cultured MCF-7 cells. The asterisks represent significant difference ($P < 0.05$, student's t test). The error bars represent standard deviation ($n = 3$). MCF-7 cells and spheroids were treated with various concentrations of Dox for 24 h.

spheroids was quantified by analyzing the stacks of confocal microscopy images, with live/dead staining. The cell viability of 2D cultured MCF-7 cells was measured by MTT assay. As shown in Fig. 5, MCF-7 monolayer cells and spheroids were treated with a series of Dox concentrations (0, 0.1, 1, and 10 μg ml^{-1}) for 24 hours. The results showed a dose-dependent effect in which a corresponding decline in the spheroid viability was related with an increasing Dox concentration. The spheroids were more resistant than 2D cells at 0.1 and 1 μg mL^{-1} of Dox similar to that reported for other spheroids and *in vivo* tissues.[43,45] Many factors were involved for this phenomenon such as drug penetration, cell–cell contact, cell-cycle distribution and varying microenvironments (such as pH, extracellular matrix) within spheroids.[21,46,47]

Conclusions

We have demonstrated a simple, low-cost and versatile 3D electrospinning fabrication method using spherical ice as a template. By controlling the size and distance of the spherical ice, we have created a 3D wPCL fibrous mat by electrospinning technology to improve the stability of aqueous droplets. By making the ice into cubic and triangular shapes, the fibrous mat with other controllable patterned architectures can be produced. Owing to the improved stability of aqueous droplets on wPCL fibrous mats, the 3D electrospun material from spherical ice was suitable for a tumor spheroid culture by the hanging drop method. We also proved that our materials were adequate for drug screening tests. We believe that these platforms would find application in future studies on not only the tumor spheroid culture but also on micro-tissue formation for tissue engineering research.

Acknowledgements

The authors would like to thank the National Natural Science Foundation of China for financial support (21305083, 21675108, 21335005) and the Fundamental Research Funds for the Central Universities (GK201603028).

References

1 S. Agarwal, J. Wendorff and A. Greiner, *Adv. Mater.*, 2009, **21**, 3343–3351.
2 L. Wu, J. Zang, L. Lee, Z. Niu, G. Horvatha, V. Braxtona, A. Wibowo, M. Bruckman, S. Ghoshroy, H.-C. Loye, X. Li and Q. Wang, *J. Mater. Chem.*, 2011, **21**, 8550–8557.
3 A. Formhals, *US Pat.*, 1975504, 1934.
4 D. Li and Y. Xia, *Nano Lett.*, 2003, **3**, 555–560.
5 D. Reneker and I. Chun, *Nanotechnology*, 1996, **7**, 216–223.
6 M. Ma, R. Hill, J. Lowery, S. Fridrikh and G. Rutledge, *Langmuir*, 2005, **21**, 5549–5554.
7 D. Yang, X. Niu, Y. Liu, Y. Wang, X. Gu, L. Song, R. Zhao, L. Ma, Y. Shao and X. Jiang, *Adv. Mater.*, 2008, **20**, 4770–4775.
8 Y. Son, W. Kim and H. Yoo, *Arch. Pharmacal Res.*, 2014, **37**, 69–78.
9 H. Ahvaz, H. Mobasheri, B. Bakhshandeh, N. Shakhssalim, M. Naji, M. Dodel and M. Soleimani, *J. Nanosci. Nanotechnol.*, 2013, **13**, 4736–4743.
10 W. Teo and S. Ramakrishna, *Nanotechnology*, 2006, **17**, R89–R106.
11 B. Sun, Y.-Z. Long, F. Yu, M.-M. Li, H.-D. Zhang, W.-J. Lia and T.-X. Xu, *Nanoscale*, 2012, **4**, 2134–2137.
12 S. Lee, S. Cho, M. Kim, G. Jin, U. Jeong and J. Jang, *ACS Appl. Mater. Interfaces*, 2014, **6**, 1082–1091.
13 Y. Yokoyama, S. Hattori, C. Yoshikawa, Y. Yasuda, H. Koyama, T. Takato and H. Kobayashi, *Mater. Lett.*, 2009, **63**, 754–756.
14 M. McClure, P. Wolfe, D. Simpson, S. Sell and G. Bowlin, *Biomaterials*, 2012, **33**, 771–779.
15 W. Song, D. An, D. Kao, Y. Lu, G. Dai, S. Chen and M. Ma, *ACS Appl. Mater. Interfaces*, 2014, **6**, 7038–7044.
16 J. Xie, M. R. MacEwan, W. Z. Ray, W. Liu, Y. D. Siewe and Y. Xia, *ACS Nano*, 2010, **4**, 5027–5036.
17 D. Zhang and J. Chang, *Nano Lett.*, 2008, **8**, 3283–3287.
18 Q. Cheng, B. L.-P. Lee, K. Komvopoulos and S. Li, *Biomacromolecules*, 2013, **14**, 1349–1360.
19 M. F. Leong, M. Z. Rasheed, T. C. Lim and K. S. Chian, *J. Biomed. Mater. Res., Part A*, 2009, **91**, 231–240.
20 M. Simonet, O. D. Schneider, P. Neuenschwander and W. J. Stark, *Polym. Eng. Sci.*, 2007, **47**, 2020–2026.
21 A. Minchinton and I. Tannock, *Nat. Rev. Cancer*, 2006, **6**, 583–592.
22 F. Pampaloni, E. Reynaud and E. Stelzer, *Nat. Rev. Mol. Cell Biol.*, 2007, **8**, 839–845.
23 L. Kunz-Schughart, J. Freyer, F. Hofstaedter and R. Ebner, *J. Biomol. Screening*, 2004, **9**, 273–285.
24 C. Hagios, A. Lochter and M. Bissell, *Philos. Trans. R. Soc., B*, 1998, **353**, 857–870.

25 V. M. Weaver, O. W. Petersen, F. Wang, C. A. Larabell, P. Briand, C. Damsky and M. J. Bissell, *J. Cell Biol.*, 1997, **137**, 231–245.
26 C. Dubessy, J. Merlin, C. Marchal and F. Guillemin, *Crit. Rev. Oncol. Hematol.*, 2000, **36**, 179–192.
27 Y. Peck and D.-A. Wang, *Expert Opin. Drug Delivery*, 2013, **10**, 369–383.
28 T. Goodwin, T. Prewett, D. Wolf and G. Spaulding, *J. Cell. Biochem.*, 1993, **51**, 301–311.
29 G. Lee, P. Kenny, E. Lee and M. Bissell, *Nat. Methods*, 2007, **4**, 359–365.
30 I. Zervantonakis, S. Chung, R. Sudo, M. Zhang, J. Charest and R. Kamm, *Int. J. Micro-Nano Scale Transp.*, 2010, **1**, 27–36.
31 Y. Gao, D. Majumdar, B. Jovanovic, C. Shaifer, P. Lin, A. Zijlstra, D. Webb and D. A. Li, *Biomed. Microdevices*, 2011, **13**, 539–548.
32 A. Ivascu and M. Kubbies, *J. Biomol. Screening*, 2006, **11**, 922–932.
33 M. Oliveira, A. Neto, C. Correia, M. Rial-Hermida, C. Alvarez-Lorenzo and J. Mano, *ACS Appl. Mater. Interfaces*, 2014, **6**, 9488–9495.
34 Y.-C. Tung, A. Hsiao, S. Allen, Y. Torisawa, M. Ho and S. Takayama, *Analyst*, 2010, **136**, 473–478.
35 A. Hsiao, Y.-C. Tung, C.-H. Kuo, B. Mosadegh, R. Bedenis, K. Pienta and S. Takayama, *Biomed. Microdevices*, 2012, **14**, 313–323.
36 E. Fennema, N. Rivron, J. Rouwkema, C. Blitterswijk and J. Boer, *Trends Biotechnol.*, 2013, **31**, 108–115.
37 G. Zhang, X. Zhang, M. Li and Z. A. Su, *ACS Appl. Mater. Interfaces*, 2014, **6**, 1729–1733.
38 L. Wang, B. Peng and Z. Su, *Langmuir*, 2010, **26**, 12203–12208.
39 D. Li and Y. Xia, *Adv. Mater.*, 2004, **16**, 1151–1170.
40 G. L. Tylor and A. D. Mcewan, *J. Fluid Mech.*, 1965, **22**, 1–15.
41 S. Saha, X. Duan, L. Wu, P. K. Lo, H. Chen and Q. Wang, *Langmuir*, 2012, **28**, 2028–2034.
42 S. Feng, X. Duan, P.-K. Lo, S. Liu, X. Liu, H. Chen and Q. Wang, *Integr. Biol.*, 2013, **5**, 768–777.
43 W. Guo, X. Loh, E. Tan, J. Loo and V. Ho, *Mol. Pharmaceutics*, 2014, **11**, 2182–2189.
44 T.-H. Kim, C. Mount, W. Gombotz and S. Pun, *Biomaterials*, 2010, **31**, 7386–7397.
45 T. Zhong, F. Xu, J. Xu, L. Liu and Y. Chen, *Biomed. Pharmacother.*, 2015, **69**, 317–325.
46 L. Kunz-Schughart, *Cell Biol. Int.*, 1999, **23**, 157–161.
47 M. Erlanson, E. Daniel-Szolgay and J. Carlsson, *Cancer Chemother. Pharmacol.*, 1992, **29**, 343–353.